Scientific Research Publishing

World Journal of Condensed Matter Physics, 2026, 16(4), 178-201
https://www.scirp.org/journal/wjcmp
ISSN Online: 2160-6927
ISSN Print: 2160-6919

Theoretical Estimation of the Thermophysical Properties of Cd-Pb Liquid Alloys at Different Temperatures

Rajendra Prasad Chaudhary[1], Prakash Ranjan Deen[2], Soni Kumari[3], Ajay Kumar Pandey[3], Jagdhar Mandal[4*], Indu Shekhar Jha[1]

[1]Department of Physics, Mahendra Morang Adarsh Multiple Campus, Biratnagar, T.U., Nepal
[2]Department of Physics, Purnea College, Purnia, Purnea University, Purnia, India
[3]Department of Physics, Purnea University, Purnia, India
[4]University Department of Physics, Tilka Manjhi Bhagalpur University, Bhagalpur, India
Email: r.p.chaudhary028@gmail.com; talk2deen@gmail.com; sonikrisharma2411@gmail.com; akpphysics01@gmail.com; *jmandal1284@gmail.com; isjha12345@gmail.com

How to cite this paper: Chaudhary, R.P., Deen, P.R., Kumari, S., Pandey, A.K., Mandal, J. and Jha, I.S. (2026) Theoretical Estimation of the Thermophysical Properties of Cd-Pb Liquid Alloys at Different Temperatures. *World Journal of Condensed Matter Physics*, **16**, 178-201.
https://doi.org/10.4236/wjcmp.2026.164010

Received: October 7, 2026
Accepted: November 22, 2026
Published: November 25, 2026

Copyright © 2026 by author(s) and Scientific Research Publishing Inc.
This work is licensed under the Creative Commons Attribution International License (CC BY 4.0).
http://creativecommons.org/licenses/by/4.0/

Open Access

Abstract

The analytical expressions deduced in the framework of quasi-lattice theory are utilized to calculate the excess Gibbs free energy of mixing, Gibbs free energy of mixing, activity, enthalpy of mixing, entropy of mixing and concentration fluctuations of Cd-Pb liquid alloys at 773 K. The theoretical results are in well agreement with correlated experimental data available in the literature. The optimization procedure in the substructure of quasi-lattice theory is employed to predict the concentration dependence of the excess free energy of mixing, activity, concentration fluctuations, short-range order parameter, excess stability function and diffusivity ratio of Cd-Pb melts at different temperatures. Again, Butler model in conjunction with quasi-lattice theory and optimization procedure is employed to investigate the concentration and temperature dependency of the surface concentration, surface tension and surface concentration fluctuations of Cd-Pb melts. The results advocates that Cd-Pb melt is a feebly segregating system and the segregating nature of system declines with the elevation of temperature from 673 to 1000 K. Further, the theoretical results indicate the possibility of the transition from segregation to the ordering behaviour of Cd-Pb melts at 1185 K.

Keywords

Quasi-Lattice Theory, Gibbs Free Energy of Mixing, Concentration Fluctuations, Excess Stability Function, Surface Tension

1. Introduction

The Cd-Pb liquid alloy is a segregating system [1] [2] in which there is a tendency of like atoms association as the nearest neighbours. The properties of mixing of Cd-Pb melts at 773 K such as free energy of mixing, G_M and excess entropy of mixing, S_M^{XS} exhibit asymmetry about the concentration, $C = 0.5$ whereas the excess free energy of mixing, G_M^{XS}, entropy of mixing, S_M and enthalpy of mixing, H_M are symmetric relative to the concentration. In the entire concentration region, $0.0 \le C \le 1.0$, the values of G_M^{XS} and H_M are positive which refers to the segregating nature of Cd-Pb melts at 773 K [1]. Similarly, the concentration dependence of the activity of Cd and Pb *i.e.* a_{Cd} and a_{Pb} demonstrate the positive departure from Raoult's law which indicates the segregating character of Cd-Pb melts at 773 K. The interesting behaviour of Cd-Pb melts attracted the attentiveness of many researchers [3]-[6] to explore the thermophysical properties of Cd-Pb melts. Odusote *et al.* [5] have employed Quasi-chemical approximation model to study the thermodynamic functions namely G_M, S_M, H_M and a_{Cd}, and structural functions such as concentration fluctuations, $S_{CC}(0)$ and short-range order parameter (SRO), α_1, and transport property like diffusivity ratio, $\frac{D_M}{D_{id}}$ of Cd-Pb melts at 773 K. The bulk properties like G_M, S_M, H_M, a_{Cd}, a_{Pb}, $S_{CC}(0)$ and α_1, surface properties such as surface concentration, C_i^s as well as surface tension, σ and transport properties namely $\frac{D_M}{D_{id}}$ and viscosity, η of Cd-Pb melts at 773 K have been analysed by simple statistical model [6]. However, the excess stability function, E^{XS}, surface concentration fluctuations, $S_{CC}^s(0)$ as well as the thermophysical properties of Cd-Pb melts at different temperatures are not investigated. Therefore, the theoretical exploration of Cd-Pb system becomes very important.

Therefore in present work, the thermophysical behaviour of Cd-Pb melts at different temperatures is explored in the light of mixing properties like G_M^{XS}, G_M, S_M, H_M, a_{Cd}, a_{Pb}, $S_{CC}(0)$, α_1, E^{XS}, C_i^s, σ, $S_{CC}^s(0)$ and $\frac{D_M}{D_{id}}$ on employing of quasi-lattice theory (QLT) [2] [7]. In the past, QLT has been successfully applied to analyse the thermophysical properties of several segregating binary alloys e.g. Zn-Sn, Al-Sn, Na-K, Ag-Cu, Al-Zn, Cd-Sn [7]-[12].

2. Formalism

The quasi-lattice theory (QLT) [7] is utilized to deduce the analytical equations for the thermodynamic functions as well as structural functions of a molten binary system at a specified temperature. The theory assumes the coupled effects of the size ratio and enthalpic along with entropic contributions to the thermodynamic behavior of the molten binary mixture.

2.1. Thermodynamic Functions: Free Energy of Mixing, G_M, Activity, $a_i\left(i \equiv A,B\right)$, Entropy of Mixing, S_M and Enthalpy of Mixing, H_M of the Binary Liquid Alloys

Assume one mole of a binary mixture (A-B) consisting of N_A (=NC) atoms of A and N_B (=N(1-C)) atoms of B occupying n_A and n_B numbers of lattice sites respectively with $C$and (1-C) representing the concentrations of the species A and B respectively. The size and shape of the constituent atoms A and B are different and there is the existence of short-range interactions between them.

The QLT [2] provides an expression for G_M when $Z \to \infty$ as enunciated by Guggenheim [13] where, Zstands for the coordination number *i.e.*

$$\frac{G_M}{RT} = C_A \ln\left(1-\beta\right) + C_B \ln\beta + C_A \beta W \tag{1}$$

$$\text{with} \quad \beta = \frac{\gamma C_B}{C_A + \gamma C_B} \quad \text{and} \quad W = n_A\left(\frac{\omega}{K_B T}\right) \tag{2}$$

where, T= temperature of the system (in Kelvin),R= molar gas constant, $C_A = C$, $C_B = 1-C$, W= order energy parameter, K_B = Boltzmann constant, $\gamma = \frac{V_B}{V_A}$ $\left(V_A < V_B\right)$ *i.e.* the size ratio and, ω is the interchange energy given by

$$\omega = \varepsilon_{AB} - \left(\frac{\varepsilon_{AA} + \varepsilon_{BB}}{2}\right) \tag{3}$$

where, ε_{ii}, ε_{jj} and $\varepsilon_{ij}\left(i \equiv A, j \equiv B\right)$ indicate the bond strengths.

It is necessary to point out that the first two terms on R. H.S. of equation (1) refer to the entropic effect whereas third term stands for the enthalpic contribution to G_M of the A-B molten system.

The excess free energy of mixing, G_M^{XS} of A-B molten system is represented by

$$\frac{G_M^{XS}}{RT} = \frac{G_M}{RT} - \frac{G_M^{id}}{RT} = \frac{G_M}{RT} - \left(C_A \ln C_A + C_B \ln C_B\right) \tag{4}$$

where, G_M^{id} = the free energy of mixing of the ideal solution.

Now, the thermodynamic activities a_A and a_B for the species A and B of A-B solution are expressed respectively as [2]

$$RT \ln a_A = G_M + a_A C_B\left(\frac{\partial G_M}{\partial C_A}\right) \tag{5a}$$

$$RT \ln a_B = G_M + a_B C_A\left(\frac{\partial G_M}{\partial C_B}\right) \tag{5b}$$

Equations (5) and (1) provide

$$\ln a_A = \ln\left(1-\beta\right) + \beta\left(\frac{\gamma-1}{\gamma}\right) + \beta^2 W \tag{6a}$$

$$\ln a_B = \ln\beta - \left(1-\beta\right)\left(\gamma-1\right) + W\gamma\left(1-\beta\right)^2 \tag{6b}$$

For A-B solution, the S_M is given by [2]

$$S_M = -\left(\frac{\partial G_M}{\partial T}\right)_P$$

$$\frac{S_M}{R} = \left[C_B \ln\beta + C_A \ln(1-\beta) + C_B\beta\left(W + \frac{\partial W}{\partial T}\right)\right] \text{ [using equation (1)]} \quad (7)$$

The H_M of the molten A-B system is represented by [2]

$$H_M = G_M + TS_M$$

$$\frac{H_M}{RT} = \frac{G_M}{RT} + \frac{S_M}{R}$$

$$\frac{H_M}{RT} = -C_A\beta T\left(\frac{\partial W}{\partial T}\right) \text{ (using equations (1) and (7)} \quad (8)$$

2.2. Structural Properties: Concentration Fluctuations, $S_{CC}(0)$, Short-Range Order (SRO) Parameter, α_1 and Excess Stability Function, E^{XS} of the Binary Solution

The microscopic functions such as $S_{CC}(0)$ [14] [15] and α_1, [16] [17] are useful to describe the nature as well as degree of atomic arrangement in the binary molten system. The $S_{CC}(0)$ in terms of G_M is expressed as

$$S_{CC}(0) = RT\left(\frac{\partial^2 G_M}{\partial C^2}\right)^{-1}_{T,P,N} \quad (9)$$

Equations (1) and (9) provide

$$S_{CC}(0) = \frac{C_A C_B}{1 - C_A C_B\{f(\gamma, W)\}} \quad (10)$$

where, $f(\gamma, W) = \left[\frac{\left\{2\gamma^2 W - (\gamma-1)^2(C_A + \gamma C_B)\right\}}{(C_A + \gamma C_B)^3}\right]$ (11)

Again in terms of activity, $S_{cc}(0)$ may be expressed as [15]

$$S_{CC}(0) = C_B a_A\left(\frac{\partial^2 G_M}{\partial C_A^2}\right)^{-1}_{T,P,N} = C_A a_B\left(\frac{\partial^2 G_M}{\partial C_B^2}\right)^{-1}_{T,P,N} \quad (12)$$

It is remarkable that $S_{cc}(0)$ computed from equation (12) is treated as the experimental value of $S_{cc}(0)$ for a binary liquid alloy.

For $\gamma = 1$ and $W = 0$, $f(\gamma, W) = 0$ (from equation (11)) and hence equation (10) provides

$$S_{cc}^{id}(0) = C_A C_B = C(1-C) \quad (13)$$

It is noted that $f(\gamma, W) < 0$ *i.e.* negative (from equation (11)), for $\gamma > 1$ and $W = 0$, hence from equation (10) $S_{CC}(0) < S_{CC}^{id}(0)$ which refers to the ordering behavior of the binary liquid alloys. Again, $S_{CC}^{id}(0) > S_{CC}(0)$ (from equation (10)), when $f(\gamma, W) < 0$ *i.e.* negative (from equation (11)) for all values of γ and $W < 0$ (*i.e.* negative). This also refers to the ordering character of the binary molten system. Further from equation (11), $f(\gamma, W) > 0$ *i.e.* positive, if $W > 0$

and hence $S_{CC}(0) > S_{CC}^{id}(0)$ (from equation (10)) which refers to the segregating behavior of the binary liquid alloys.

Now SRO, α_1 in the closest neighboring shell of a binary molten system is given by [2] [12]

$$\alpha_1 = \frac{(S-1)}{S(Z-1)+1} \quad \text{with} \quad S = \frac{S_{CC}(0)}{S_{CC}^{id}(0)} \tag{14}$$

where, Z = the coordination number (usually taken to be 10).

The excess stability function, E^{XS} proposed by Darken [18] is directly linked to $S_{CC}(0)$ as [2] [9]

$$E^{XS} = \frac{RT}{S_{CC}(0)} - \frac{RT}{C_A C_B} \tag{15}$$

Obviously, for segregating behaviour of alloys, $S_{CC}(0) > S_{CC}^{id}(0)$, E^{XS} is negative while E^{XS} becomes positive for ordered alloys because $S_{CC}^{id}(0) > S_{CC}(0)$.

2.3. Surface Properties: Surface Concentration, C_i^s, Surface Tension, σ and Surface Concentration Fluctuations, $S_{cc}^s(0)$ of the Molten Binary System

Butler model [19] has been employed in conjunction with QLT [2] to explore the surface tension of a binary A-B system. The expression for surface tension, σ of a binary solution is given by

$$\sigma = \sigma_A + \left(\frac{\tilde{G}_A^{E,s} - \tilde{G}_A^{E,b}}{S_A}\right) + \frac{RT}{S_A}\ln\left(\frac{C_A^S}{C_A}\right) \tag{16a}$$

$$= \sigma_B + \left(\frac{\tilde{G}_B^{E,s} - \tilde{G}_B^{E,b}}{S_B}\right) + \frac{RT}{S_B}\ln\left(\frac{C_B^S}{C_B}\right) \tag{16b}$$

where $\sigma_i (i \equiv A, B)$ = the surface tension of the component, i, $\tilde{G}_i^{E,b}$ and $\tilde{G}_i^{E,s} (i \equiv A, B)$ = the partial excess free energy of component i in the bulk and at the surface respectively. $S_i (i \equiv A, B)$ = the molar surface area of the ith component and, C_i and C_i^s = the bulk and surface concentrations, respectively. Now $S_i (i \equiv A, B)$ is expressed as [11]

$$S_i (i \equiv A, B) = 1.091 V_i^{\frac{2}{3}} N_A^{\frac{1}{3}} \tag{17}$$

Where N_A = Avogadro's number and V_i = the atomic volume of the component, i of the binary solution.

The partial excess free energy of the component, i in the bulk, $\tilde{G}_i^{E,b}$ is represented by [2]

$$\tilde{G}_i^{E,b} = RT \ln \gamma_i \quad \text{with} \quad \gamma_i = \frac{a_i}{c_i} (i \equiv A, B) \tag{18}$$

where, γ_i = the activity coefficient of the component, i in the bulk.

The relation between $\tilde{G}_i^{E,b}$ and $\tilde{G}_i^{E,s}$ is represented by [2]

$$\tilde{G}_i^{E,s} = \lambda \tilde{G}_i^{E,b} \tag{19}$$

where, $\lambda = \frac{Z^s}{Z}$, the ratio of the surface coordination number, Z^s to the bulk coordination number Z [20] and λ varies from 0.50 to 0.84 [21].

The surface concentration fluctuations, $S_{cc}^s(0)$ is very important parameter to explain the atomic arrangement at the surface of a binary melt. Mathematically, $S_{cc}^s(0)$ is represented by [22] [23]

$$S_{cc}^s(0) = \frac{C_A^s C_B^s}{\left[1 + \frac{Z^S}{2\lambda^s\left(1-\lambda^s\right)}\right]} \tag{20}$$

$$\text{with } \lambda^s = \left[1 + 4C_A^s C_B^s \left\{\exp\left(\frac{2W}{Z^s K_B T}\right) - 1\right\}\right]^{\frac{1}{2}} \tag{21}$$

$$C_A^s C_B^s = S_{CC}^{id,s}(0) \tag{22}$$

which denotes the ideal surface concentration fluctuations.

2.4. Transport Properties: Diffusivity Ratio, $\frac{D_M}{D_{id}}$

The transport properties *i.e.* diffusivity, Dis very fruitful to explain the mixing characteristics of the binary melts at the microscopic level. The diffusivity ratio for the binary solution is expressed as [2] [23] [24].

$$\frac{D_M}{D_{id}} = \frac{S_{CC}^{id}(0)}{S_{CC}(0)} \tag{23}$$

where, D_M and D_{id} = the mutual diffusion coefficient for a molten binary system and intrinsic diffusion coefficient of an ideal system respectively. In terms of self-diffusion coefficients *i.e.* D_A and D_B for the components A and B respectively, D_{id} is represented by

$$D_{id} = C_A D_B + C_B D_A \tag{24}$$

From equation (23), it is clear that $\frac{D_M}{D_{id}} > 1$ for the ordered alloys [7] [24] whereas $\frac{D_M}{D_{id}} < 1$ for the segregating alloys [7] [25].

2.5. Optimization Procedure

The optimization procedure [2] [8] [9] is an important tool for the prediction of the thermophysical characteristics of the binary melts in the temperature regions where the exact experimental measurements are difficult. For this purpose, Redlich-Kister (R-K) approach is applied to determine a suitable set of polynomials to describe the temperature and concentration dependency of the mixing properties

of the binary melts.

The temperature and concentration dependence of G_M^{XS} is represented as [2]

$$G_M^{XS}(c,T) = c(1-c)\sum_{l=0}^{m} K_l(T)(2c-1)^l \tag{25}$$

$$\text{where, } K_l(T) = A_l T + B_l T + C_l T + \ln T + D_l T^2 \tag{26}$$

The coefficient $K_l\left(l = 0,1,2,3,\cdots\right)$ depends on the temperature in the similar fashion as G (free energy of mixing) depends on the temperature *i.e.*

$$G = A + BT + CT + \ln T + DT^2 + ET^{-1} \tag{27}$$

The partial excess free energy for the constituents A and B may be expressed respectively as [2] [8] [9]

$$\tilde{G}_{M,A}^{XS} = (1-C)^2 \sum_{l=0}^{m} K_l(T)\left[(1+2l)C - (1-C)\right](2C-1)^{l-1} \tag{28a}$$

$$\tilde{G}_{M,B}^{XS} = (1-C)^2 \sum_{l=0}^{m} K_l(T)\left[(1+2l)C - (1-C)\right](2C-1)^{l-1} \tag{28b}$$

The G_M^{XS} of a binary liquid alloy is represented by

$$G_M^{XS} = C\tilde{G}_A^{XS} + (1-C)\tilde{G}_B^{XS} \tag{29}$$

The partial excess free energy of the component, $i\ (i \equiv A,B)$ and activity coefficient, γ_i are related as

$$\tilde{G}_i^{XS} = RT\ln\gamma_i \left(i \equiv A,B\right) \tag{30}$$

The activity *i.e.* $a_i\left(i \equiv A,B\right)$ and activity coefficients are related as

$$a_i = \gamma_i C_i \tag{31}$$

3. Results and Discussions

3.1. Bulk Properties: G_M, $a_i\left(i \equiv A,B\right)$, S_M, H_M, $S_{CC}(0)$, α_1 and E^{XS} for Cd-Pb Melts at 773 K

The analytical equations deduced in the framework of QLT have been employed to compute the bulk properties of Cd-Pb melts at 773 K. The investigative equation (1) shows that for the computation of G_M, the values of model parameters *i.e.* W and γ are required. The size ratio *i.e.* $\gamma\left(=\frac{V_{Pb}}{V_{Cd}}\right)$ is determined using the values of the volumes of Cd and Pb *i.e.* V_{Cd} and V_{Pb} at 773 K. For this, the values of V_{Cd} and V_{Pb} at the corresponding melting points [26] are utilised in the relation given below

$$V_i(T) = V_i(T_m)\left[1 + \alpha_i\left(T - T_m\right)\right] \tag{32}$$

where, $i(=Cd,Pb)$, α_i = coefficient of thermal expansion of the ith component in the liquid state and T_m = melting temperature (in K), T = 773 K. The value of $\gamma\left(=\frac{V_{Pb}}{V_{Cd}}\right)$ is found to 1.3798. It is necessary to note that γ = 1.3798 is not suitable for the computation of the concentration dependency of G_M for Cd-

Pb molten alloys at 773 K whatever the value of W be. Therefore, γ is also assumed as a model parameter [8] [27].In present case, the value of γ may be slightly changed in order to obtain the better results for G_M [8] [9]. The parameter, W is ascertained by the successive method [10] [28] [29] on applying the experimental data of G_M for Cd-Pb melts at 773 K in equation (1). The reasonable values of W and γ are found to be $W = 1.15$ and $\gamma = 1.45$.

These values of W and γ are utilized for the computations of the bulk properties of Cd-Pb melts at 773 K in order to maintain the consistency.

The theoretical values of $\frac{G_M}{RT}$ as a function of concentration of Cd exhibit excellent harmony with the experimental values [1] as shown in **Figure 1**. The observed asymmetry in G_M for Cd-Pb melts at 773 Kis well explained having minima *i.e.* $\frac{G_M}{RT}\left(\min^{m}\right) = -0.3740$ (Theory) and −0.3654 (Experiment) at $C_{Cd} = 0.4$ with an error of 2.35%. The magnitude of $\frac{G_M}{RT}$ indicates that Cd-Pb melt at 773 K is a feebly interacting in nature [30].

The theoretical results of $\frac{G_M^{XS}}{RT}$ for Cd-Pb melts at 773 K achieved from equation (5) exhibit the excellent agreement with the experimental data [1] as cited in **Figure 1**. It is observed that the values of $\frac{G_M^{XS}}{RT}$ are positive in the entire composition range from C_{Cd} = 0.1 to 0.9with maxima at C_{Cd} = 0.5 *i.e.* $\frac{G_M^{XS}}{RT}\left(\max^{m}\right) = 0.3231$ (Theory) and 0.3283 (Experiment) having an error of 1.58%. Thus, the observed symmetry in G_M^{XS} has been successfully reproduced.

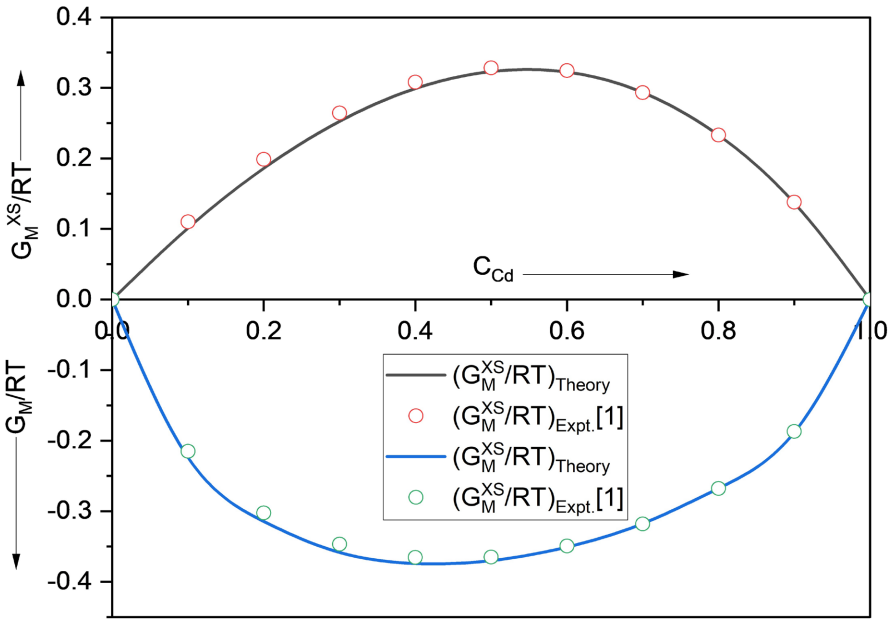

Figure 1. $\frac{G_M^{XS}}{RT}$ and $\frac{G_M}{RT}$ versus C_{Cd} for Cd-Pb melts at 773 K.

Figure 2 demonstrates the concentration-dependent values of a_{Cd} and a_{Pb} i.e activities of Cd and Pb respectively for Cd-Pb molten alloys at 773 K determined from equations (6a) and (6b). The $a_i\left(i \equiv Cd, Pb\right)$ versus concentration isotherm indicates an excellent agreement between theoretical data and correlated experimental data [1] for Cd-Pb melts at 773 K. The positive departure of $a_i\left(i \equiv Cd, Pb\right)$ from ideal mixing shows the segregating behavior of Cd-Pb molten system at 773 K. It is remarkable to note that the thermodynamic activity of a binary solution is measured directly by the experiments. Thus, the agreement between the theoretical values and correlated experimental values of a_{Cd} and a_{Pb}, provides the validity to the values of W and γ.

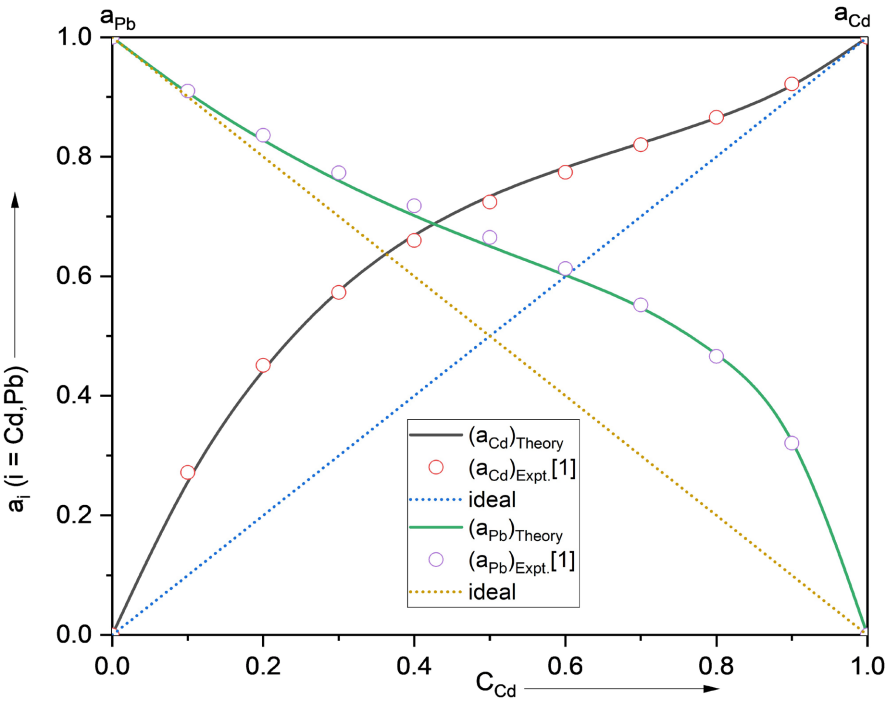

Figure 2. $a_i\left(i = Cd, Pb\right)$ versus C_{Cd} for Cd-Pb melts at 773 K.

The equations (7) and (8) are employed to obtain the values of $\frac{S_M}{R}$ and $\frac{H_M}{RT}$ respectively for Cd-Pb molten alloys at 773 K relative to the concentration of Cd. For this, the temperature derivative of W *i.e.* $\frac{\partial W}{\partial T}$ is required. It should be pointed out that the temperature derivative of γ is negligibly small [11]. In order to ascertain the value of $\frac{\partial W}{\partial T}$, the method of successive approximation is employed on using the experimental data of S_M [1] in equation (7) for Cd-Pb system at 773 K. The value of $\frac{\partial W}{\partial T}$ is found to be -0.00182 K^{-1}. **Figure 3** exhibits a reasonable agreement between the theory and experiment [1] for both S_M and H_M for Cd-Pb melts at 773 K with maxima at C_{Cd} = 0.5 *i.e.* $\frac{S_M}{R}\left(\max^m\right)$ = 0.7863 (Theory) and 0.7789

(Experiment) with an error of 0.95%, and $\frac{H_M}{RT}\left(\max^{m}\right)$ 0.4163 (Theory) and 0.4136 (Experiment) with an error of 0.65%. Thus, the observed symmetry in both S_M and H_M have been successfully explained by the present theoretical analysis.

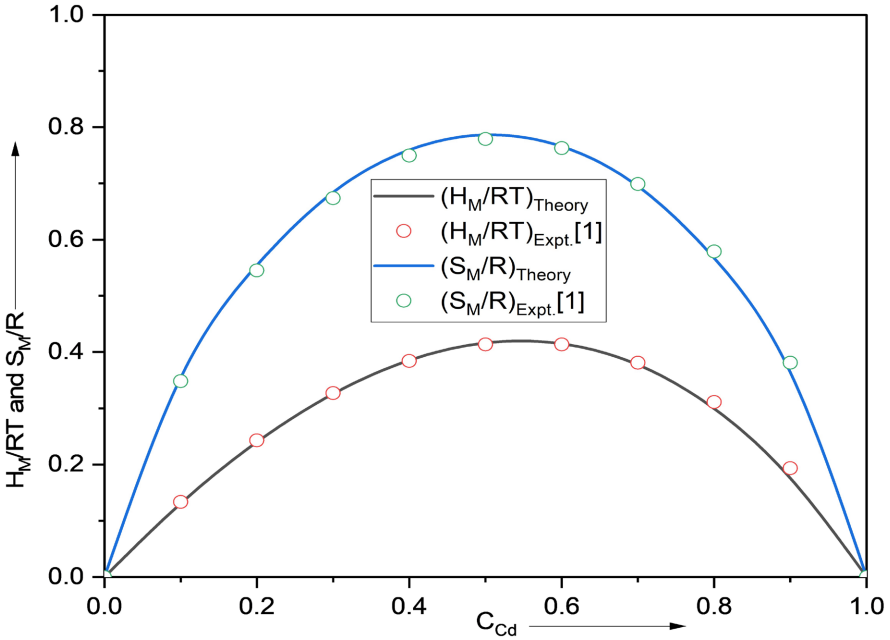

Figure 3. $\frac{H_M}{RT}$ and $\frac{S_M}{R}$ versus C_{Cd} for Cd-Pb melts at 773 K.

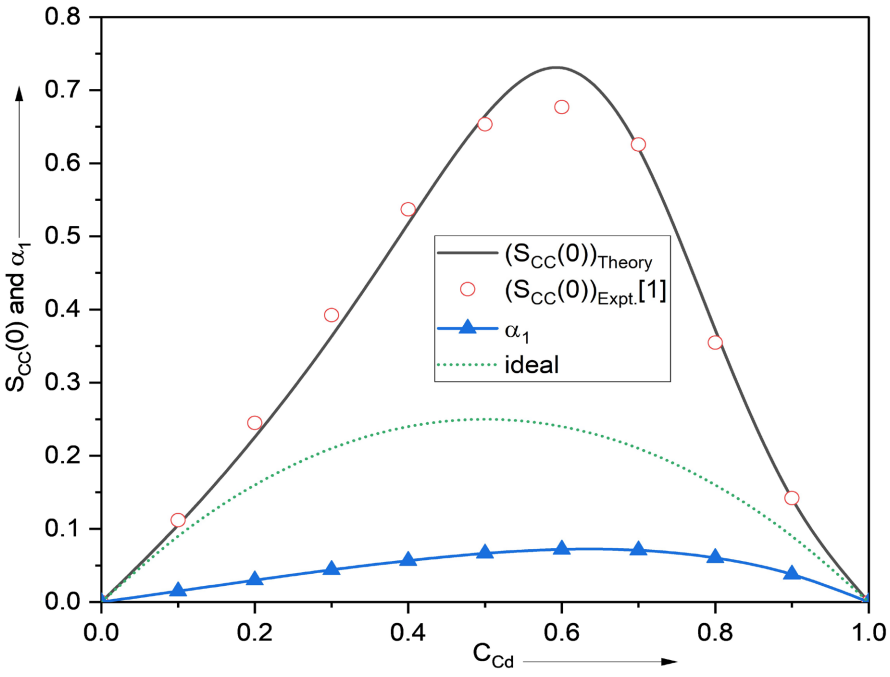

Figure 4. $S_{CC}(0)$ and α_1 versus C_{Cd} for Cd-Pb melts at 773 K.

Equations (10) and (11) are used to compute the concentration dependence of

$S_{CC}(0)$ for Cd-Pb molten alloys at 773 K. The $S_{CC}(0)-C$ isotherm is depicted in Figure 4 and exhibits good agreement between theory and experiment [1]. At each concentration of Cd, $S_{CC}(0) > S_{CC}^{id}(0)$ which indicates the segregating behavior *i.e.* like atoms (Cd-Cd or Pb-Pb) association as the closest neighbors in Cd-Pb molten system at 773 K [2] [10]. The values of $S_{CC}(0)$ are maximum *i.e.* 0.731 (Theory) and 0.677 (Experiment) both at $C_{Cd} = 0.6$ having an error of 7.98%. This indicates the asymmetric character of Cd-Pb alloys at 773 K.

The concentration dependency of SRO, α_1 is depicted in Figure 5 for Cd-Pb liquid alloys at 773 K. At each concentration of Cd, α_1 is positive with maximum value of 0.0720 at $C_{Cd} = 0.6$ which refers to the segregation in Cd-Pb liquid alloys at 773 K [2] [10]. Again, the magnitude of α_1 signifies that the Cd-Pb liquid alloys at 773 K is a weakly segregating system.

In order to explore the characteristics of molten Cd-Pb system at 773 K, the excess stability function, E^{XS} is predicted from equation (15) on applying the theoretical values of $S_{CC}(0)$. The $E^{XS}-C$ isotherm presented in Figure 5 demonstrates that E^{XS} is negative in the entire region of concentration *i.e.* C_{Cd} = 0.1 to 0.9 which confirms the segregating behavior of Cd-Pb molten system at 773 K similar to Al-Sn molten alloys at 973 K [8].

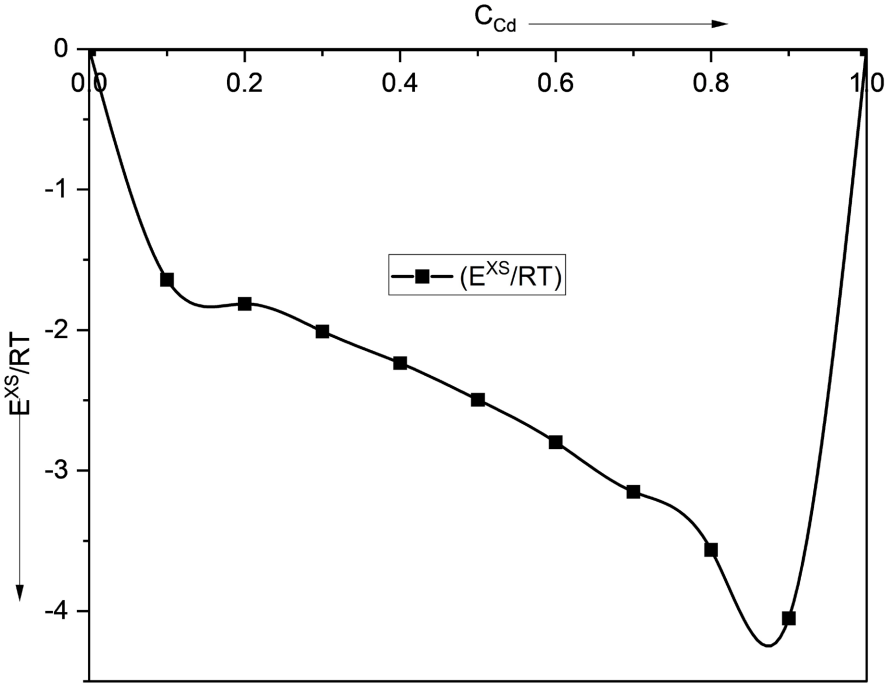

Figure 5. $\frac{E^{XS}}{RT}$ versus C_{Cd} for Cd-Pb melts at 773 K.

3.2. Results for G_M^{XS}, Activity, $S_{CC}(0)$, α_1 and E^{XS} of Cd-Pb Melts at Various Temperatures

In recent years, optimization procedure is adopted as an important tool [2] [8] [9] [12] for the exploration of the thermophysical properties of binary solutions like

Al-Sn, Na-K, Cd-Sn etc on employing the theoretical data of G_M^{XS}. The optimization coefficients for a given binary system are evaluated by least square method. The optimized coefficients are further utilized for the prediction of thermophysical characteristics of a binary system at various temperatures. It is important to note that the optimization procedure is very useful for the prediction of thermophysical properties where no experimental data is available in the literature.

The optimization procedure in conjunction with QLT is used for the prediction of the theoretical findings of G_M^{XS} for Cd-Pb system at different temperatures. The concentration dependency of the partial excess free energy for both the components *i.e.* $A = Cd$ and $B = Pb$ is determined at different temperatures from equations (28a) and (28b) respectively. For this purpose, the optimized coefficients A_l, B_l, C_l and D_l are required to obtain the values of $K_l \left(l = 0,1,2,3\right)$ from equation (29). The equation (30) is used to ascertain the needed values of $K_l \left(l = 0,1,2,3\right)$ on using data of G_M^{XS} for Cd-Pb system at various temperatures. Therefore, in order to explore the thermophysical properties of Cd-Pb melts at various temperatures, the data of G_M^{XS} for Cd-Pb melts at various temperatures are required. Since there is scarce of experimental data of G_M^{XS} in the literature for Cd-Pb melts at various temperatures, hence the theoretical data of G_M^{XS} are employed as suggested earlier [7].

In order to compute the G_M^{XS} at various temperatures, the values of model parameters at various temperatures for Cd-Pb molten system are required. The values of $W(T)$ at desired temperature can be computed by the relation [8] [9]

$$W\left(T\right) = W\left(T_0\right) + \frac{\partial W}{\partial T}\left(T - T_0\right) \tag{33}$$

where,

$T_0 = 723$ K

T = desired temperature in K

$$\frac{\partial W}{\partial T} = -0.00182 \text{ K}^{-1}$$

$$W\left(T_0\right) = 1.15$$

It is notable that the change in size ratio, γ is significantly small [8] [10] with the change in temperature under consideration. Thus, the γ is kept constant during entire calculation for Cd-Pb melts as taken earlier [8]-[10]. The estimated values of W at 673 K, 773 K, 873 K and 973 K are listed in **Table 1**.

Table 1. Values for interaction energy parameter.

Temperature (in K)	Energy parameter (W)
673	1.332
773	1.150
873	0.968
973	0.785

Obviously, the value of interaction energy parameter W declines with the rise in temperature which is similar to earlier findings [8]-[10].

Equations (32) and (33) are utilised to determine $\frac{G_M^{XS}}{RT}$ at 673 K, 773 K, 873 K and 973 K for Cd-Pb melts relative to the concentration. Again, equations (29) and (30) are utilized to compute the optimized coefficients, A_l, B_l, C_l and D_l (l = 0, 1, 2 and 3) by the least square method, which are mentioned in **Table 2**. It is to be noted that once the values of A_l, B_l, C_l and D_l are known, they are frequently utilized to determine the optimized values of the thermodynamic functions at any desired temperature.

Table 2. Optimized coefficients for Cd-Pb melts.

Values of l	$A_l\left(\mathrm{J\cdot mole^{-1}}\right)$	$B_l\left(\mathrm{J\cdot mole^{-1}\cdot K^{-1}}\right)$	$C_l\left(\mathrm{J\cdot mole^{-1}\cdot K^{-1}}\right)$	$D_l\left(\mathrm{J\cdot mole^{-1}\cdot K^{-2}}\right)$
0	364134.14502	−5658.43069	839.74686	−0.49992
1	67889.53512	−1054.99685	156.56325	−0.09932
2	12735.49541	−197.91149	29.36992	−0.01747
3	2349.50016	−36.51191	5.41829	−0.00322

The equations (28a), (28b) and (29) are utilized to ascertain the concentration dependence of $\frac{G_M^{XS}}{RT}$ at 673 K, 773 K, 900 K and 1000 K for Cd-Pb melts which are presented in **Figure 6**. The experimental data of $\frac{G_M^{XS}}{RT}$ [1] are also incorporated in **Figure 6**, which exhibit good agreement with the optimized data of $\frac{G_M^{XS}}{RT}$. For the understanding the deviation between the experimental data and theoretical data accurately, the average standard deviation, S have been determined from thee relation

$$S = \pm\sqrt{\frac{1}{n}\sum_{1}^{n}\left(X_{Th} - X_{Expt}\right)^2} \tag{34}$$

where, X_{Th} and X_{Expt} = the theoretical and experimental data of the concerned thermodynamic function.

The computed value of the average standard deviation for $\frac{G_M^{XS}}{RT}$ of Cd-Pb melts at 773 K is found to be sufficiently small *i.e.* $S = \pm 0.0062$ which explains the reliability of the optimization procedure.

Figure 6 shows that the values of $\frac{G_M^{XS}}{RT}$ is positive in the composition region, C_{Cd} = 0.1 to 0.9 at each temperature and concentration which is an indication of the segregating character of Cd-Pb melts in the temperature region, 673-1000 K. Again, the segregation of Cd-Pb molten system decreases with the elevation of temperature because $\frac{G_M^{XS}}{RT}$ exhibits declination with the upgradation of temperature. Again, the peak-position of G_M^{XS} is maintained in the temperature region,

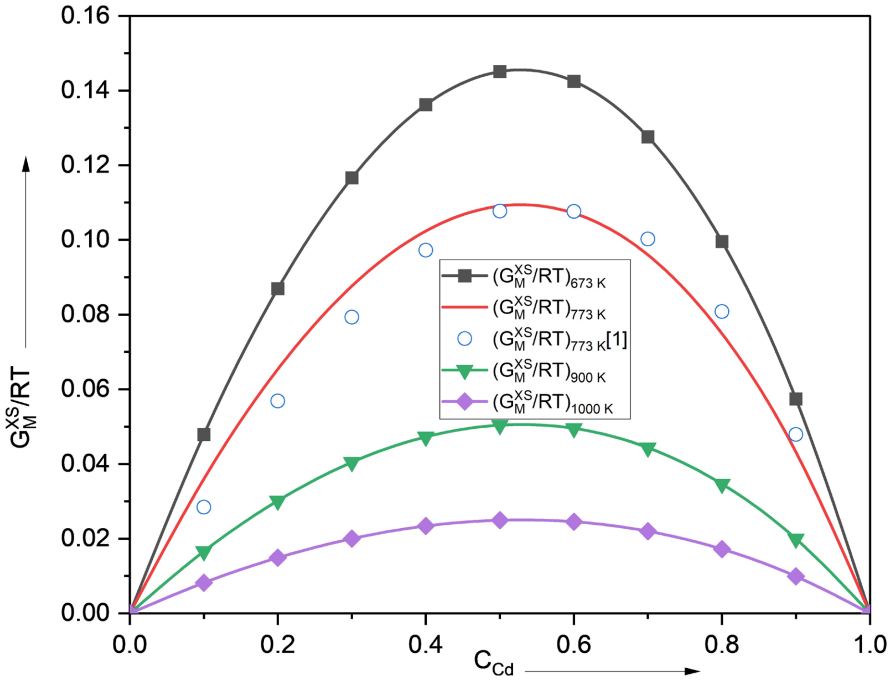

Figure 6. $\frac{G_M^{XS}}{RT}$ versus C_{Cd} for Cd-Pb melts at 673 K, 773 K, 900 K and 1000 K.

673 - 1000 K because the value of $\frac{G_M^{XS}}{RT}$ is maximum at C_{Cd} = 0.5 *i.e.* 0.4330 at 673 K, 0.3231 at 773 K, 0.2563 at 900 K and 0.1969 at 1000 K. Thus, the segregating in Cd-Pb melt appears to be maximum at the equiatomic composition in the temperature region 673-1000 K.

The theoretical values of a_{Cd} and a_{Pb} calculated from equations (34) and (35) for Cd-Pb melts at 673 K, 773 K, 900 K and 1000 K are depicted in **Figure 7** relative to composition of Cd. The experimental data for a_{Cd} and a_{Pb} at 773 K [1] are also included in in **Figure 7**. The theoretical and experimental values of a_{Cd} and a_{Pb} for Cd-Pb melts at 773 K exhibit well agreement. The average standard deviations determined from equation (34) for a_{Cd} and a_{Pb} of Cd-Pb melts at 773 K are ± 0.0077 and ± 0.0081 respectively, which are very small. This indicates the reliability of the optimization procedure.

In the temperature-region 673 -1000 K, both a_{Cd} and a_{Pb} possess the positive departures from the ideal mixing behaviour and the magnitude of the positive departure decreases with the rise in temperature. This corresponds to the degradation in the homo-coordination existing in Cd-Pb molten system with the elevation of temperature. However, the degradation of the segregating character of Cd-Pb system is comparatively weak in the temperature region from 673 - 1000 K.

3.3. Results for $S_{CC}(0)$, α_1 and E^{XS} for Cd-Pb Melts at Different Temperatures

Equation (12) is utilized to determine the values of $S_{CC}(0)$ for Cd-Pb melts on employing the theoretical data of a_{Cd} and a_{Pb} at 673 K, 773 K, 900 K and 1000 K.

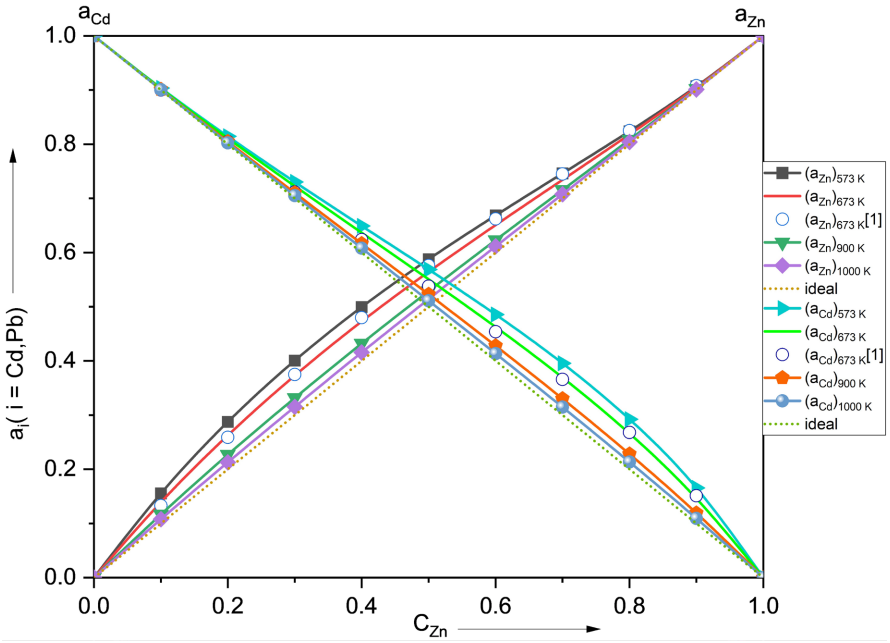

Figure 7. $a_i\ (i = Cd, Pb)$ versus C_{Cd} for Cd-Pb melts at 673 K, 773 K, 900 K and 1000 K.

The theoretical results for Cd-Pb melts of $S_{CC}(0)$ at 673 K, 773 K, 900 K and 1000 K are cited in **Figure 8** as a function of composition of Cd along with the correlated experimental data at 773 K [1] as well as $S_{cc}^{id}(0)$. It should be pointed out that $S_{CC}(0)$ demonstrate a well agreement between the theory and experiment for Cd-Pb melts at 773 K having maxima i.e 0.733 (Theory) and 0.677 (Experiment) both at C_{Sn} = 0.6. The $S_{CC}(0)-C$ isotherms indicate that the theoretical values of $S_{CC}(0)$ deviates positively from $S_{cc}^{id}(0)$ at each concentration for Cd-Pb melts at the temperatures from 673 K to 1000 K. Again, the magnitude of the positive deviations declines at each concentration with the rise in the temperature. This signifies that the segregation in Cd-Pb melts decreases with the elevation of temperature from 673 K to 1000 K. The values of $S_{CC}(0)$ computed beyond 1000 K are also included in **Figure 8**. It is remarkable that in the composition range *i.e.* $0.0 \le C_{Cd} \le 1.0$, the theoretical values of $S_{CC}(0)$ are almost equivalent to $S_{cc}^{id}(0)$ at 1185 K. On further increasing the temperature, the theoretical value of $S_{CC}(0)$ gradually decreases and becomes less than $S_{cc}^{id}(0)$ at 1200K and 1220 Kin the composition region *i.e.* $0.1 \le C_{Cd} \le 0.9$. However at each temperature, $S_{CC}(0)$ is maximum at C_{Cd} = 0.6 *i.e.* 2.433 at 673 K, 0.733 at 773 K, 0.677 at 900 K, 0.514 at 1000 K, 0.236 at 1185 K, 0.226 at 1200 K and 0.212 at 1220 K which indicate the asymmetric behavior of Cd-Pb system in the temperature region, 673-1220 K. Therefore, the present theoretical investigation advocates that there is a probability of the transition from segregating to ordering character of Cd-Pb melts at the temperature about 1185 K. This theoretical predictions is based on the linear dependency of the interaction parameter on temperature. The similar result is observed for the segregating system like Al-Sn, Na-K and Cd-Sn

melts [8] [9] [12]. Again, there is a likelihood of maximum segregation about C_{Cd} = 0.6 in Cd-Pb melts.

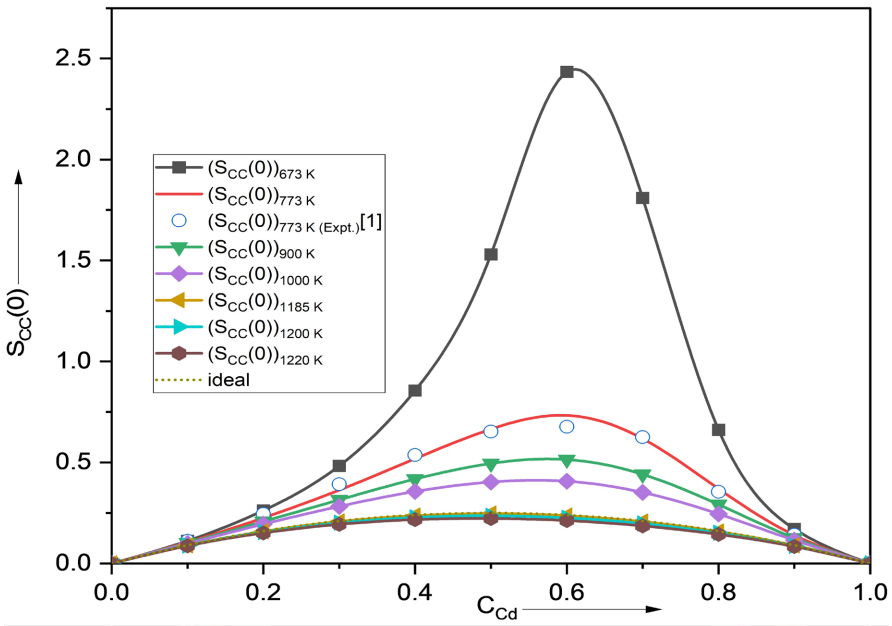

Figure 8. $S_{CC}(0)$ versus C_{Cd} for Cd-Pb melts at 673 K, 773 K, 900 K, 1000 K, 1185 K, 1200 K and 1220 K.

The theoretical data of α_1 for Cd-Pb melts at 673 K, 773 K, 900 K and 1000 K 1185 K, 1200 K and 1220 K are presented in **Figure 9** with respect to the composition of Cd. It is mention that the experimental data of α_1 are not available in the literature for comparison. The $\alpha_1 - C$ isotherms signify that at each concentration, the α_1 is positive with maximum value at C_{Cd} = 0.6 such as 0.0991, 0.0721, 0.0563 and 0.0427 at 673 K, 773 K, 900 K and 1000 K respectively for Cd-Pb melts indicating the segregating character of the system. At 1185 K, the α_1 is almost equal to zero in the entire concentration range. On further raising the temperature, α_1 becomes negative having values −0.2233 and −0.22 at 1200 K and 1220 K respectively.

This indicates that Cd-Pb melts show asymmetric nature with respect to concentration, and the segregation in Cd-Pb melts gradually decreases with the elevation of the temperature from 673-1000 K. Again, the magnitude of the α_1 refers to weakly segregating behavior of Cd-Pb melts. Further, the present theoretical prediction indicates that there may be transformation of segregation to the ordering nature of Cd-Pb melts at the temperature about 1185 K.

The theoretical results for E^{XS} calculated from equation (15) for Cd-Pb system relative to the concentration of Cd at 673 K, 773 K, 900 K,1000 K, 1185 K, 1200 K and 1220 K are shown in **Figure 10.** It is found that $\frac{E^{XS}}{RT}$ possesses negative values at each concentration of Cd from 0.1 to 0.9 at 673 K, 773 K, 900 K and 1000 K of which magnitude decreases with the rise in temperature.

This advocates that the segregation in Cd-Pb molten system gradually decreases

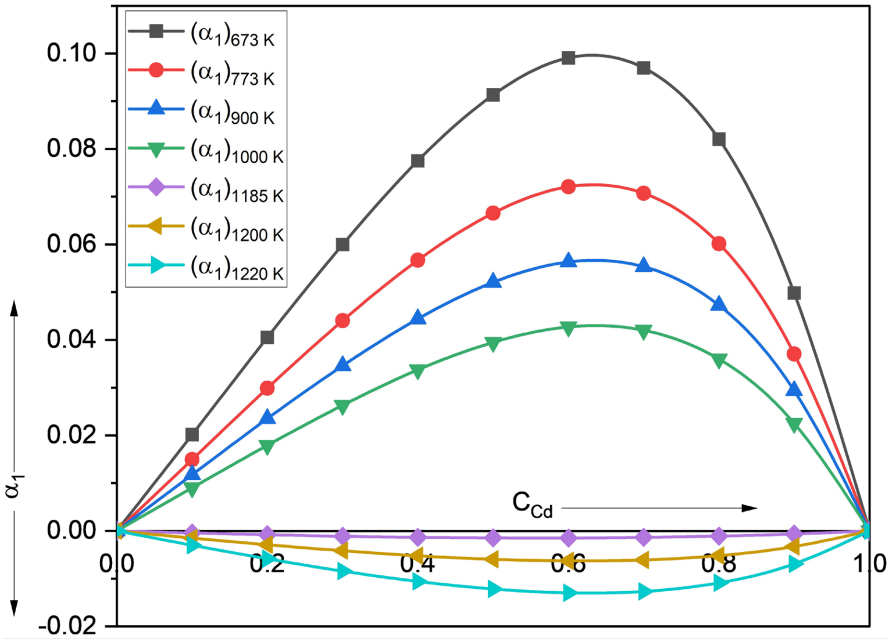

Figure 9. α_1 versus C_{Cd} for Cd-Pb melts at 673 K, 773 K, 900 K, 1000 K, 1185 K, 1200 K and 1220 K.

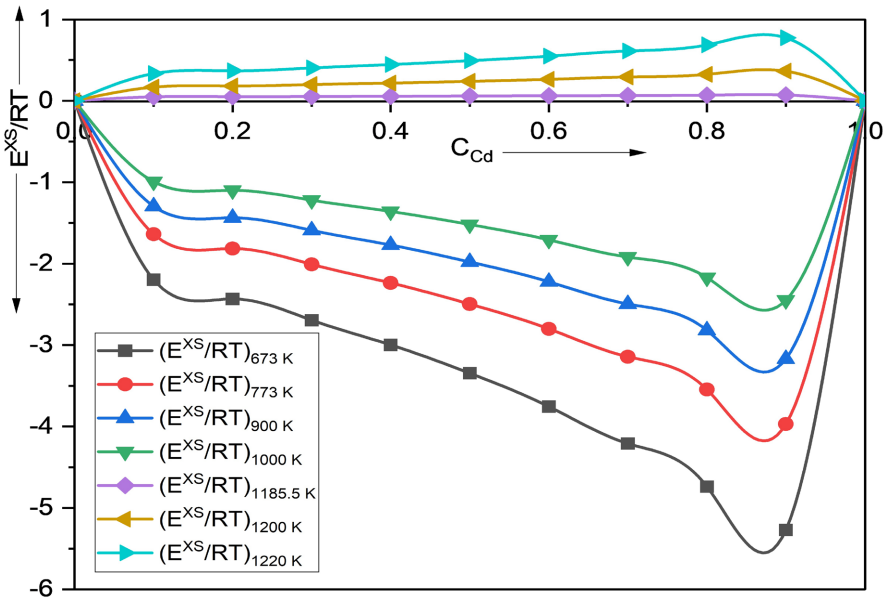

Figure 10. $\frac{E^{XS}}{RT}$ versus C_{Cd} for Cd-Pb melts at 673 K, 773 K, 900 K,1000 K, 1185 K, 1200 K and 1220 K.

with the elevation of temperature. The theoretical data of $\frac{E^{XS}}{RT}$ is almost equal to zero at each concentration of Cd when the temperature is elevated to 1185 K which refers to the ideal mixing of Cd-Pb melts. The theoretical values for $\frac{E^{XS}}{RT}$ of Cd-Pb melts at 1200 K and 1220 K, indicate the positive values in the entire composition

range of Cd. The values of $\frac{E^{XS}}{RT}$ increases with the elevation of temperature from 1200 K and 1220 K. This signifies the ordering character of the Cd-Pb melts. Thus, the present theoretical analysis reveals that there may be the probability of the transition from segregating to ordering character of Cd-Pb melts at the temperature about 1185 K. Similar results are found for Na-K and Cd-Sn melts[9] [12].

3.4. Surface Properties: C_i^s, σ and $S_{CC}^s(0)$ of Binary Melts

Equations (16a) and (16b) are utilized to determine the surface tension, σ for Cd-Pb melts at 773 K. For this purpose, $\tilde{G}_i^{E,b}$, $\tilde{G}_i^{E,s}$, S_i and $C_i^s\left(i \equiv Cd, Pb\right)$ are required. On determining the activity coefficient, $\gamma_i\left(i \equiv Cd, Pb\right)$ from relation $\gamma_i = \frac{a_i}{c_i}$, the equation (18) is utilized to determine the values of $\tilde{G}_i^{E,b}$ as a function of concentration of Cd for Cd-Pb melts at 773 K. Taking λ = 0.82, $\tilde{G}_i^{E,s}\left(i \equiv Cd, Pb\right)$ is determined from equation (19). For the determination of $S_i\left(i \equiv Cd, Pb\right)$, V_i is required which is determined from the relation

$$V_i(T) = \frac{M_i}{\rho_i(T)} \tag{35a}$$

$$\text{with } \rho_i(T) = \rho_i(T_m) + \frac{\partial \rho_i}{\partial T}(T - T_m) \tag{35b}$$

where, $i \equiv (Cd, Pb)$, T= 773 K, T_m = the melting temperature of the ith component, M_i = the atomic mass of component i, $\rho_i(T_m)$ and $\rho_i(T)$ = densities of the ith component at the melting temperature and 773 K respectively, and $\frac{\partial \rho_i}{\partial T}$ = the temperature coefficient of density for i^{th} component . The input data have been tabulated in **Table 3** [26].

Table 3. The physical properties of Cd and Pb [26].

Metal	M.P.	Atomic mass	Density	Tempr. Coefft. of density
	(T_m in K)	(M in Kg)	(ρ in Kgm^{-3})	($\frac{\partial \rho}{\partial T}$ in $Kgm^{-3}K^{-1}$)
Cd	594.05	0.11241	8010	−1.22
Pb	600.61	0.20719	10670	−1.32

The value of the surface tension of pure i^{th} component $(i = Cd, Pb)$ at 773 K is calculated on employing the equation

$$\sigma_i(T) = \sigma_i(T_m) + \frac{\partial \sigma_i}{\partial T}(T - T_m) \tag{36}$$

where,

$\frac{\partial \sigma_i}{\partial T}$ = temperature coefficient of surface tension of ith component

The required parameters for pure Cd and Pb are listed in **Table 4**.

Table 4. Surface tension and coefficient of surface tension for Cd and Pb [26].

Metal	Surface tension (σ in mNm^{-1})	Coefficient of surface tension ($\frac{\partial\sigma}{\partial T}$ in $mNm^{-1}K^{-1}$)
Cd	570	−0.26
Pb	458	−0.13

The equations (18) and (19) are used to determine the values of the partial excess free energy of both the components Cd and Pb in the bulk and at the surface for the required temperatures on using $\lambda = 0.82$ [21].

The equations (16a) and (16b) are solved simultaneously to determine the values of C_{Cd}^{s} and σ for Cd-Pb melts relative to the bulk concentration of Cd *i.e.* $C_{Cd}^{b} = C_{Cd}$. The concentration dependence of C_{Cd}^{s} at 673 K, 773 K, 900 K and 1000 K for Cd-Pb melts is mentioned in **Figure 11** as a function of C_{Cd}.

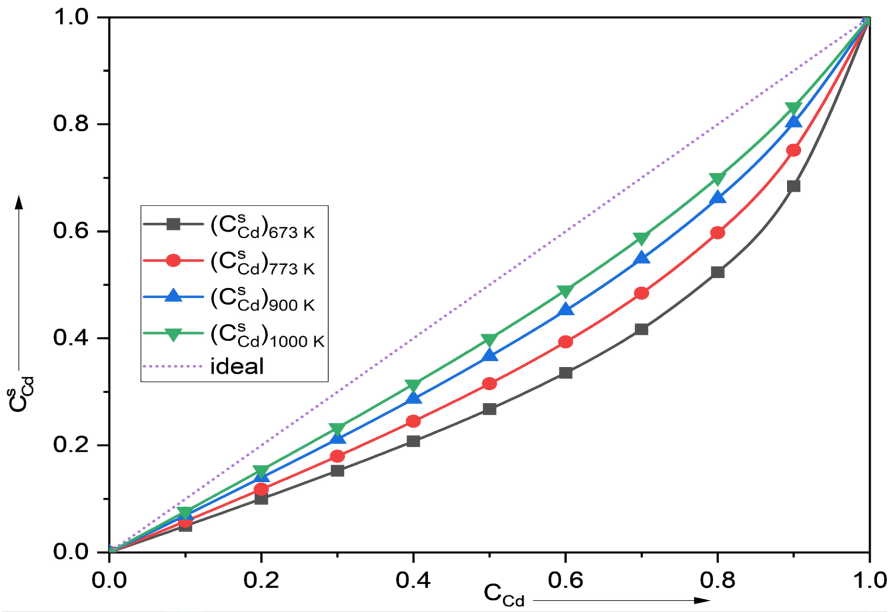

Figure 11. C_{Cd}^{s} versus C_{Cd} for Cd-Pb melts at 673 K, 773 K, 900 K and 1000 K.

It is evident that C_{Cd}^{s} deviates negatively from the ideal surface concentration in the entire concentration region at each temperature under consideration for Cd-Pb melts. This signifies that at the surface the number of Cd-atoms is less than that of Pb-atoms *i.e.* Pb-atoms aggregate at the surface with the elevation of the bulk concentration of Cd. Again, the negative deviation of C_{Cd}^{s} decreases with the elevation in temperature from 673 - 1000 K. This illustrates the declination of the aggregation of Pb-atoms at the surface with the rise in temperature in Cd-Pb melts which is identical to the results for In-Zn system [23] [31].

The theoretical data of σ relative to the bulk concentration of Cd for Cd-Tl melts at 673 K, 773 K, 900 K and 1000 K are displayed in **Figure 12**. Obviously, the surface tension of Cd-Pb melts increases with the addition of Cd-atoms in Cd-Pb melts at each temperature under consideration. This is due to the fact that Cd has

larger value of surface tension than that of Pb. Again, $\sigma - C_{Cd}$ isotherms indicate that the surface tension of Cd-Pb melts decreases with the increase of temperature in the whole bulk composition region of Cd. It is pointed out that the theoretical data of σ are not compared with the experimental data due to unavailability in the literature.

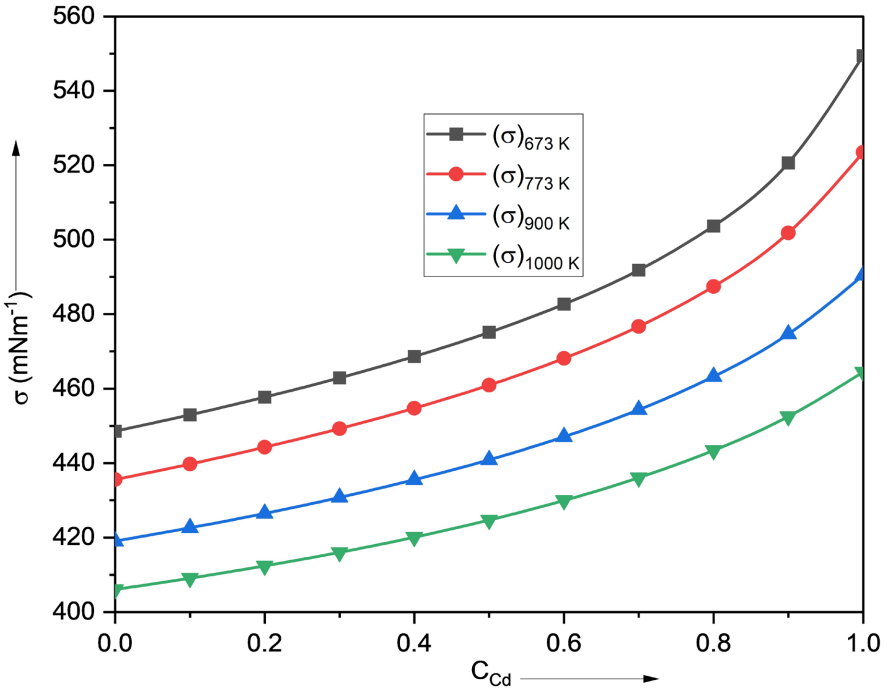

Figure 12. σ versus C_{Cd} for Cd-Pb melts at 673 K, 773 K, 900 K and 1000 K.

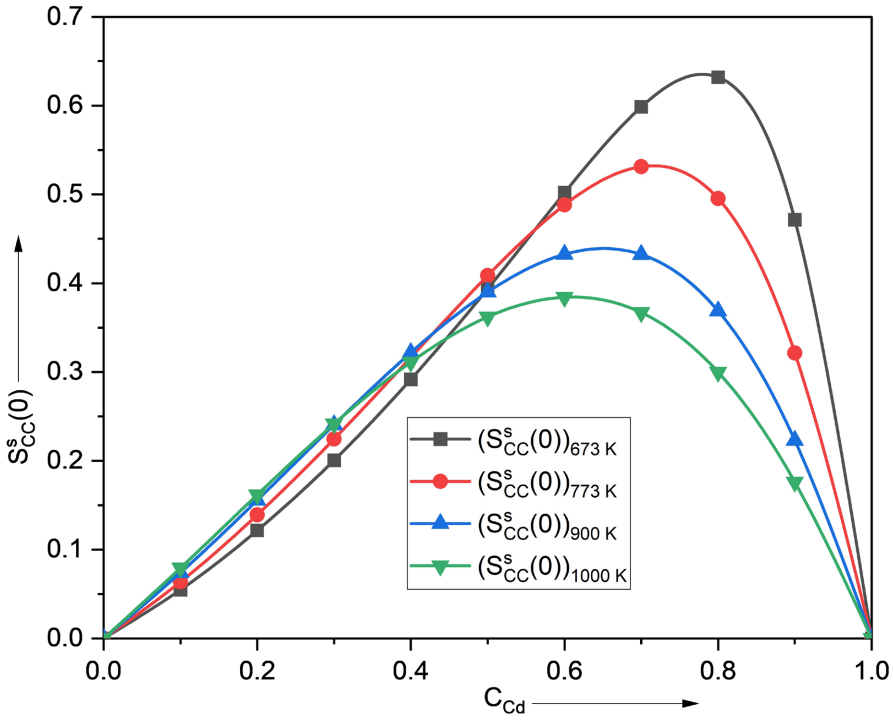

Figure 13. $S^s_{CC}(0)$ versus C_{Cd} for Cd-Pb melts at 673 K, 773 K, 900 K and 1000 K.

The theoretical values of $S_{CC}^{s}(0)$ evaluated from equations (20) and (21) for Cd-Pb mixture at 673 K, 773 K, 900 K and 1000 K are mentioned in Figure 13. Obviously, $S_{CC}^{s}(0)$ increases with the bulk composition of Cd to a maximum value and then decreases at each temperature. The maximum values of $S_{CC}^{s}(0)$ are 0.632 at C_{Cd} = 0.8 for 673 K, 0.531 at C_{Cd} = 0.7 for 773 K, 0.433 at C_{Cd} = 0.6 for 900 K, and 0.384 at C_{Cd} = 0.6 for 1000 K. In the region $0.6 \le C_{Cd} \le 1.0$, the values of $S_{CC}^{s}(0)$ decrease at each concentration with the rise in temperature from 673 K to 1000 K indicating a declination in the segregating behavior of Cd-Pb melts. In the region $0.0 \le C_{Cd} \le 0.6$, the crossover effect is noticed. Therefore, the present theoretical results suggest that there is maximum possibility of the phase separation of Cd-Pb melts in the composition range, C_{Cd} = 0.6 to 0.8 [31].

3.5. Results for Transport Properties of Cd-Pb at Different Temperatures

The equation (23) is applied for the theoretical assessment of $\frac{D_M}{D_{id}}$ for Cd-Pb melts at 673 K, 773 K, 900 K and 1000 K. The theoretical data of $\frac{D_M}{D_{id}}$ depicted in Figure 14, shows that $\frac{D_M}{D_{id}} < 1$ at each temperature in the whole composition range of Cd, $C_{Cd} = 0.1$ to 0.9 which is a sign of segregating character of Cd-Pb molten system. Again, the magnitude of $\frac{D_M}{D_{id}}$ is elevated with the increase of temperature from

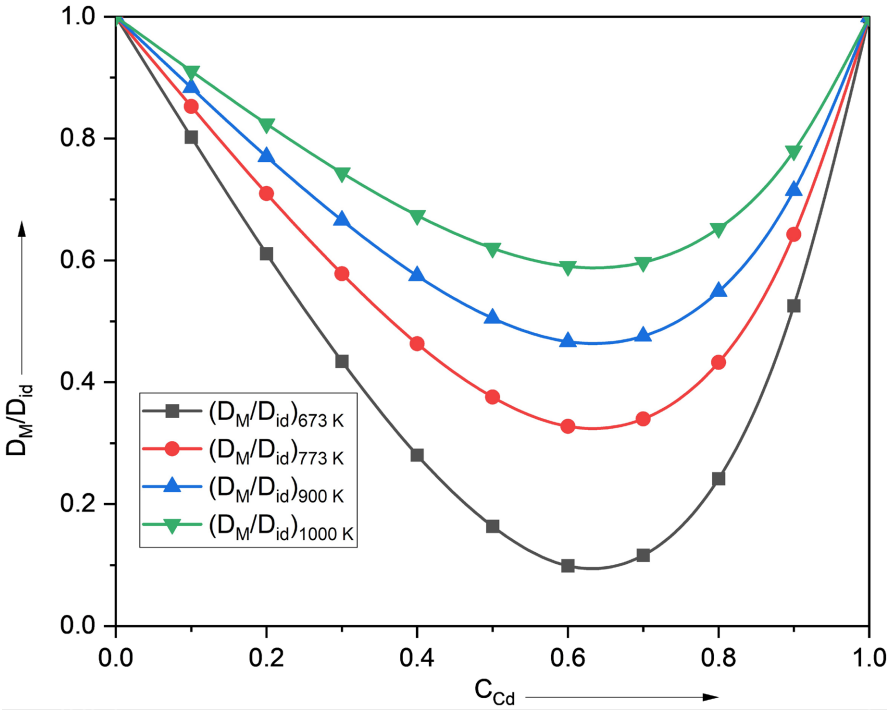

Figure 14. $\frac{D_M}{D_{id}}$ versus C_{Cd} for Cd-Pb melts at 673 K, 773 K, 900 K and 1000 K.

673 - 1000 K which signifies the decrease in the segregating nature of Cd-Pb molten system. Further, the values of $\frac{D_M}{D_{id}}$ indicate that the degree of segregation in Cd-Pb melts is small [2] and hence the system is a feebly segregating in nature.

4. Conclusions

The present theoretical investigation successfully explains the thermodynamic, structural, surface and transport properties of Cd-Pb melts at different temperatures. The theoretical data for G_M^{XS}, G_M, S_M, H_M, a_{Cd}, a_{Pb} and $S_{CC}(0)$ relative to the concentration exhibit well agreement with the correlated experimental data for Cd-Pb melts at 773 K. The concentration dependence of G_M^{XS}, a_{Cd}, a_{Pb}, $S_{CC}(0)$, α_1 and E^{XS} at 673 K, 773 K, 900 K and 1000 K predicted in the framework of QLT as well as optimized procedure reveal that Cd-Pb melt is a weakly segregating system and nature of decreases with the elevation of temperature from 673 K to1000 K. The surface properties namely C_i^s, σ and $S_{CC}^s(0)$ of Cd-Pb melts are theoretically predicted at the aforesaid temperatures on employing Butler model in conjunction with QLT and optimization procedure which indicates that Cd-Pb melt possess homo-coordination of the atoms *i.e.* pairing of Cd-Cd or Pb-Pb atoms as the nearest neighbours. Further, the concentration and temperature dependency of $S_{CC}(0)$, α_1, E^{XS} and $\frac{D_M}{D_{id}}$ suggests the likelihood of the transition from segregating to ordering nature of Cd-Pb melts at 1185 K. It should be pointed out that in the present theoretical work, the interaction parameter, W is supposed to be linearly depending upon the temperature and a constant size ratio. The transition from segregating to ordering nature of Cd-Pb melts at higher temperature requires further theoretical computations by molecular dynamics or density functional theory.

Thus, the quasi-lattice theory is a reliable approach to explain the concentration and temperature dependence of the thermophysical properties of the molten segregating alloys. However, QLT is found to be inadequate to explain the mixing behaviour of the compound forming alloys.

Author Contributions

Conceptualization: I.S. Jha and J. Mandal and A.K. Pandey; methodology: R.P. Chaudhary; validation: I.S. Jha; J. Mandal and A.K. Pandey; formal analysis: R.P. Chaudhary; investigation: P.R. Deen and SoniKumari; writing-original draft preparation: P.R. Deen and SoniKumari; writing-review and editing: R.P. Chaudhary; visualization: I.S. Jha and A.K. Pandey; supervision: J. Mandal.

Conflicts of Interest

The authors declare no conflicts of interest regarding the publication of this paper.

References

[1] Hultgren, R., Desai, P.D., Hawkins, D.T., Gleiser, M. and Kelley, K.K. (1973) Selected

Values of the Thermodynamic Properties of Binary Alloys, ASM, Metal Park, Ohio Publication Information/Link.

[2] Singh, R.N. and Sommer, F. (1997) Segregation and Immiscibility in Liquid Binary Alloys. *Reports on Progress in Physics*, **60**, 57-150. https://doi.org/10.1088/0034-4885/60/1/003

[3] Kumar, R. and Sivaramakrishnan, C.S. (1969) Stability of Liquid Pb-Cd Systems. *Journal of Materials Science*, **4**, 377-382. https://doi.org/10.1007/bf00549701

[4] Dutkiewicz, J., Moser, Z. and Zakulski, W. (1988) The Cd-Pb (Cadmium-Lead) System. *Bulletin of Alloy Phase Diagrams*, **9**, 694-701. https://doi.org/10.1007/bf02883171

[5] Odusote, Y.A., Fayose, O.O. and Odigie, P.J. (2007) Mixing Properties of X-Pb, (X=Cd, In) Liquid Binary Alloys. *Journal of Non-Crystalline Solids*, **353**, 4666-4671. https://doi.org/10.1016/j.jnoncrysol.2007.07.006

[6] Singh, B.P., Koirala, I., Jha, I.S. and Adhikari, D. (2014) The Segregating Nature of Cd-Pb Liquid Binary Alloys. *Physics and Chemistry of Liquids*, **52**, 457-470. https://doi.org/10.1080/00319104.2013.871668

[7] Shrestha, G.K., Singh, B.K., Jha, I.S., Koirala, I., Singh, B.P. and Adhikari, D. (2017) Theoretical Investigations on Thermodynamic Properties and Concentration Fluctuations of Zn-Sn Binary Liquid Alloys at Different Temperatures by Optimization Method. *Journal of the Chinese Advanced Materials Society*, **5**, 186-203. https://doi.org/10.1080/22243682.2017.1320229

[8] Shrestha, G.K., Singh, B.K., Jha, I.S., Singh, B.P. and Adhikari, D. (2017) Optimization Method for the Study of the Properties of Al-Sn Binary Liquid Alloys. *Physica B*: *Condensed Matter*, **514**, 1-7. https://doi.org/10.1016/j.physb.2017.03.005

[9] Singh, A.P., Chaudhary, R.P., Kumari, R., Jha, I.S. and Mandal, J. (2022) Stability of Nak Liquid Alloys at Different Temperatures. *Materials Today*: *Proceedings*, **66**, 2251-2258. https://doi.org/10.1016/j.matpr.2022.06.097

[10] Chaudhary, R.P., Mandal, J. and Indu Shekhar, J. (2022) Symmetries in the Properties of Mixing of AgCu Liquid Alloys at 1423 K. *Materials Today*: *Proceedings*, **49**, 2283-2287. https://doi.org/10.1016/j.matpr.2021.09.343

[11] Chaudhary, R.P., Mandal, J. and Jha, I.S. (2022) Concentration Dependence of the Bulk and Surface Properties of Liquid AlZn Alloys at 1000 K. *Materials Today*: *Proceedings*, **59**, 397-404. https://doi.org/10.1016/j.matpr.2021.11.358

[12] Singh, A.P., Chaudhary, R.P., Hussain, M.M., Mandal, J. and Jha, I.S. (2024) Theoretical Study of the Stability of CdSn Liquid Alloy at Different Temperatures. *Diffusion Foundations and Materials Applications*, **37**, 37-51. https://doi.org/10.4028/p-efgqf5

[13] Guggenheim, E.A. (1952) Mixtures: The Theory of the Equilibrium Properties of Some Simple Classes of Mixtures, Solutions and Alloys. Oxford University Press.

[14] Bhatia, A.B. and Thornton, D.E. (1970) Structural Aspects of the Electrical Resistivity of Binary Alloys. *Physical Review B*, **2**, 3004-3012. https://doi.org/10.1103/physrevb.2.3004

[15] Singh, R.N. (1987) Short-Range Order and Concentration Fluctuations in Binary Molten Alloys. *Canadian Journal of Physics*, **65**, 309-325. https://doi.org/10.1139/p87-038

[16] Warren, B.E. (1969) X-Ray Diffraction. Addition-Wesley Publishing.

[17] Cowley, J.M. (1950) An Approximate Theory of Order in Alloys. *Physical Review*, **77**,

669-675. https://doi.org/10.1103/physrev.77.669

[18] Darken, L.S. (1967) Thermodynamics of Binary Metallic Solutions. *Transactions of the Metallurgical Society of AMIE*, **239**, 80-89.

[19] Butler, J.A.V. (1932) The Thermodynamics of the Surfaces of Solutions. *Proceedings of the Royal Society of London, Series A, Containing Papers of a Mathematical and Physical Character*, **135**, 348-375. https://doi.org/10.1098/rspa.1932.0040

[20] Costa, C., Delsante, S., Borzone, G., Zivkovic, D. and Novakovic, R. (2014) Thermodynamic and Surface Properties of Liquid Co-Cr-Ni Alloys. *The Journal of Chemical Thermodynamics*, **69**, 73-84. https://doi.org/10.1016/j.jct.2013.09.034

[21] Kaptay, G. (2005) Modelling Interfacial Energies in Metallic Systems. In: *Materials Science Forum*, Trans Tech Publications Ltd., 1-10. https://doi.org/10.4028/0-87849-957-1.1

[22] Prasad, L.C. and Singh, R.N. (1991) Surface Segregation and Concentration Fluctuations at the Liquid-Vapor Interface of Molten Cu-Ni Alloys. *Physical Review B*, **44**, 13768-13771. https://doi.org/10.1103/physrevb.44.13768

[23] Anusionwu, B.C. and Ilo-Okeke, E.O. (2006) Segregation and Surface Properties of In-Zn Liquid Alloys. *Physics and Chemistry of Liquids*, **43**, 25-36. https://doi.org/10.1080/00319100420003035 27

[24] Bhagat, S.K., Chaudhary, R.P., Pandey, A.K., Mandal, J. and Jha, I.S. (2025) Thermodynamic and Structural Properties of CuSn Melts. *Applied Physics A*, **131**, Article No. 932. https://doi.org/10.1007/s00339-025-09017-5

[25] Chaudhary, R.P., Hussain, M.M., Roy, N.K., Mandal, J. and Jha, I.S. (2026) Thermophysical Properties of In-Tl Melts at 723 K. *World Journal of Condensed Matter Physics*, **16**, 73-89. https://doi.org/10.4236/wjcmp.2026.163005

[26] Iida, T. and Guthrie, R.I.L. (1988) The Physical Properties of Liquid Metals. Clarendon Press.

[27] Ilo-Okeke, E.O., Anusionwu, B.C. and Popoola, O. (2005) Thermodynamic Evaluation of Viscosity in In-Zn and Sn-Zn Liquid Alloys. *Physics and Chemistry of Liquids*, **43**, 333-342. https://doi.org/10.1080/00319100500087964

[28] Kumar, A., Jha, I.S. and Singh, B.P. (2011) Quasi-Lattice Model for the Thermodynamic Properties and Microscopic Structure of Molten Fe-Si Alloy. *Physica B: Condensed Matter*, **406**, 4338-4341. https://doi.org/10.1016/j.physb.2011.08.060

[29] Jha, I.S., Khadka, R., Koirala, R.P., Singh, B.P. and Adhikari, D. (2016) Theoretical Assessment on Mixing Properties of Liquid Tl-Na Alloys. *Philosophical Magazine*, **96**, 1664-1683. https://doi.org/10.1080/14786435.2016.1177668

[30] Bhatia, A.B. and Hargrove, W.H. (1974) Concentration Fluctuations and Thermodynamic Properties of Some Compound Forming Binary Molten Systems. *Physical Review B*, **10**, 3186-3196. https://doi.org/10.1103/physrevb.10.3186

[31] Awe, O.E. and Azeez, A.A. (2017) Temperature Dependence of the Bulk and Surface Properties of Liquid Zn-Cd Alloys. *Applied Physics A*, **123**, Article No. 363. https://doi.org/10.1007/s00339-017-0977-3